

# Bounds on Low Scale Gravity from RICE data and Cosmogenic Neutrino Flux Models

Shahid Hussain

*Bartol Research Institute, University of Delaware, Newark, DE 19716*

Douglas W. McKay

*University of Kansas Dept. of Physics and Astronomy, Lawrence KS 66045-2151, USA*

(Dated: February 8, 2020)

We explore limits on low scale gravity models set by results from the Radio Ice Cherenkov Experiment's (RICE) ongoing search for cosmic ray neutrinos in the cosmogenic, or GZK, energy range. Depending upon cosmogenic flux model, black hole formation and decay treatment, and inclusion of graviton mediated elastic neutrino processes, we find bounds in the range  $0.9 \text{ TeV} < M_D < 10 \text{ TeV}$ , where  $M_D$  is the fundamental scale of gravity. Values  $d = 5, 6$  and  $7$ , for which laboratory and astrophysical bounds on LSG models are less restrictive, lead to essentially the same limits on  $M_D$ .

PACS numbers: 96.40.Tv, 04.50.th, 13.15.+g, 14.60.Pq

## I. INTRODUCTION

The highest energy cosmic ray events range to values above  $10^5 \text{ PeV}$  [1], with hundreds of TeV equivalent center-of-mass energies. Prospects of achieving comparable energies at an accelerator laboratory are remote, at best. The opportunities for probing fundamental physics at these ultrahigh energies will be confined to cosmic rays for the foreseeable future. The weakness of neutrino interactions at currently available energies allows neutrinos to carry information to us line of sight from deep within highly energetic astrophysical sources. For the same reason, enhancements of neutrino interaction rates by new physics at ultra-high energies can be dramatic and distinctive. On the other hand, similar sized enhancements in the electromagnetic and strong interaction rates can easily be obscured. These two, unique features of neutrinos - direct propagation from source to observer and sensitivity to new physics - drive the effort to build neutrino telescopes to cover energies from fractions of an MeV to detect  $p - p$  neutrinos from the sun to thousands of PeV to detect cosmogenic neutrinos, those originating from the decays of pions created by collisions of the highest energy cosmic rays with the cosmic microwave radiation photons [2, 3].

In this paper we present bounds on new physics, specifically on the scale  $M_D$  in models of low scale gravity [4], that follow from proposed models of cosmogenic neutrino fluxes[5, 6, 7, 8] and the absence of UHE neutrino events in the Radio Ice Cherenkov Experiment (RICE) data from 2000 through 2004 [9]. Before proceeding to a description of the calculation, the results and the summary and conclusions, we sketch the essential features of the RICE detection system and the features of low scale gravity that lead to prediction of event rates in RICE that exceed those expected from neutrino interactions in the standard model (SM).

**The RICE experiment** The advantages of weakly interacting neutrinos raise the obvious question of detection. Neutrino detection is possible with some combination of large fluxes and large detector volumes. Accelerator neutrino facilities strive for high fluxes and detectors the size of large fixed target experiments. But in the energy range above a PeV, the predicted cosmogenic fluxes are extremely small and decrease rapidly with energy. the high energy end of the expected cosmogenic flux range,  $10^4 - 10^5 \text{ PeV}$ , can be characterized by the observed cosmic ray figure of 1 event per  $\text{km}^2$  per century. *Many* cubic kilometers is the effective detector volume that must be achieved.

The RICE detector concept relies on characteristics of UHE showers, radio wavelength emission from these showers, and the transmission of radio wavelengths in cold, pure ice [10]. The showers in dense media (e.g. ice), are compact, travel faster than light in the medium and are smaller in transverse size than sub-GHz frequency wavelengths. The showers develop a net excess charge at shower maximum that is about  $10^6$  electrons at a PeV, and is proportional to energy. This net charge emits *coherent* Cherenkov radiation at frequencies up to a GHz. This radiation has an attenuation length of more than a kilometer in Antarctic ice. A single radio antenna can be sensitive to neutrino induced showers within more than a  $\text{km}^3$  of ice at the highest energies; even a modest, pilot array has an effective volume,  $V_{\text{eff}}$ , of many cubic kilometers. Discussion of the recent RICE analysis can be found in Ref. [9], while more details of the full experiment are given in Refs. [11] and [12].

### Low scale gravity and UHE Cosmic Ray Neutrinos

The phenomenology of low scale gravity (LSG) [4] predicts enhanced cross sections mediated by gravity, including production of black holes in high energy particle reactions [13], [14]. Under quite general assumptions, the gravity enhanced cross sections, such as that for black hole production, are large, and grow with a power of the center of mass energy. After formation, black holes are thought to evaporate to a statistical mixture of many particles [15],

producing a characteristic signature. There is great interest in black hole production at current and future colliders as a “low energy” probe of extra dimensions [16, 17]. Yet even the LHC energies may not be large enough to reach the black hole regime [17].

A number of ultra-high energy neutrino studies take advantage of the fact that the highest energies accessible in particle physics occur not at colliders, but in cosmic rays; this is then coupled to the prediction that low scale gravity cross sections in extra dimension models, while much smaller than hadronic, can be orders of magnitude larger than standard model (SM) *neutrino* cross sections at ultra-high energies[18]. With the assumption that the collision energy dumped into a black hole is released as visible energy in air shower detectors or neutrino telescope detectors, predictions of event rates and consequent bounds on  $M_D$ , the “Planck mass” of extra-dimension gravity, have been presented for various model estimates of neutrino flux [19].

A low scale gravity effect that does not depend on the black hole dynamics is graviton exchange, producing an hadronic shower from the graviton - parton interaction in the nucleon. This is a variety of deep-inelastic, neutral-current process, and we include this in our study as well. This class of events is complementary to black hole production and decay. Though the cross sections are large, the elasticity is high, greater than  $\sim 90\%$ , so relatively little of the neutrino energy is deposited in the showers. Nonetheless, in part of the parameter space this “deep inelastic” gravity effect competes with the black hole formation.

## II. SUMMARY OF DIRECT BLACK HOLE PRODUCTION AND GRAVITON MEDITATED NEUTRINO DEEP INELASTIC SCATTERING

We present the essential components of our calculation of the number of events expected in RICE data [9] from SM, black hole, and graviton-mediated interactions . For impact parameters less than the Schwarzschild radius,  $r_S$ , the black disk, black hole cross section formula has often been adopted, which reads

$$\hat{\sigma}_{\text{BH}} \approx \pi r_S^2, \quad (1)$$

without including gray body [20], or impact parameter[21] and form factor [22], effects. Later we include a model for the impact parameter dependence for comparison. In Eq. (1),  $r_S$  is the  $4+d$  dimensional Schwarzschild radius of a black hole of mass  $M_{BH}$  [23]:  $r_S = \frac{1}{M_D} \left[ \frac{M_{BH}}{M_D} \right]^{\frac{1}{1+d}} \kappa_d$ , where  $\kappa_d = 2.1, 2.44$ , or  $2.76$  for cases  $d = 5, 6$ , or  $7$ , respectively. Here  $M_D$  is the  $4+d$  dimensional Planck mass scale of extra-dimensional physics, which is the scale we aim to explore with UHE RICE data in this study. Equation (1) is a parton level cross section, and the effective black hole mass is  $M_{BH} = \sqrt{\hat{s}}$ , with  $\hat{s} = xs$ ;  $s$  is the square of the center-of-mass energy and  $x$  is the momentum fraction of the struck parton. The corresponding cross section is given by

$$\sigma_{\nu N \rightarrow BH}(E_\nu) = \int_{x_{\min}}^1 dx \hat{\sigma}_{BH}(xs) \sum_i f_i(x, Q), \quad (2)$$

where the  $f_i(x, Q)$  are the parton distribution functions,  $x_{\min} = M_{BH0}^2/s$  or  $1/r_s^2 s$ , whichever is larger; the sum over index  $i$  accounts for different parton flavors. Here  $s = 2M_N E_\nu$ , and  $Q$  is chosen to be  $\sqrt{xs}$ . Choosing  $Q = \frac{1}{r_s}$  [16] makes insignificant difference.  $E_\nu$  is the primary neutrino energy. The choices of  $x_{\min}$  and  $Q$  are not unique, as discussed in the papers listed in Refs. [16, 17, 19]. Here  $M_{BH0}$  is a free parameter corresponding to the minimum energy needed to form a black hole.

So far we have described the simplest versions of BH formation to estimate cross sections and UHE shower rates. Many possible modifications show up when the horizon forming collision is studied in detail. A proposal by Yoshino and Nambu [21] to sharpen the horizon formation criterion is straightforward to implement [24], and we include it here to illustrate the effect on the event rates for BH production. The impact parameter dependence of the apparent horizon formation is conveniently presented as a plot of mass contained within an apparent horizon ( $M_{A.H.}$ ) vs. impact parameter. We fit the graph of  $M_{A.H.}$  vs  $b$  with a function  $M_{A.H.}(b/b_{\max} = z)$ , the mass contained within an horizon as a function of impact parameter, scaled by the impact parameter beyond which no horizon forms,  $b_{\max}$ , as in Ref. [21]. We set the lower limit of  $x$ ,  $x_{\min} = (M_{BH0})^2/M_{A.H.}^2(z)$ . The form of the cross section is still taken to be  $\sigma(\hat{s}) = \pi r_s^2(\hat{s})$ , but the threshold for BH production is raised, which accounts for c.m. energy that does not contribute to BH formation and subsequent decay to observable particles. In addition to the x-integral, the cross section now includes an average over impact parameter, taken to be weighted geometrically by the area element  $d(\pi b^2)/\pi b_{\max}^2$

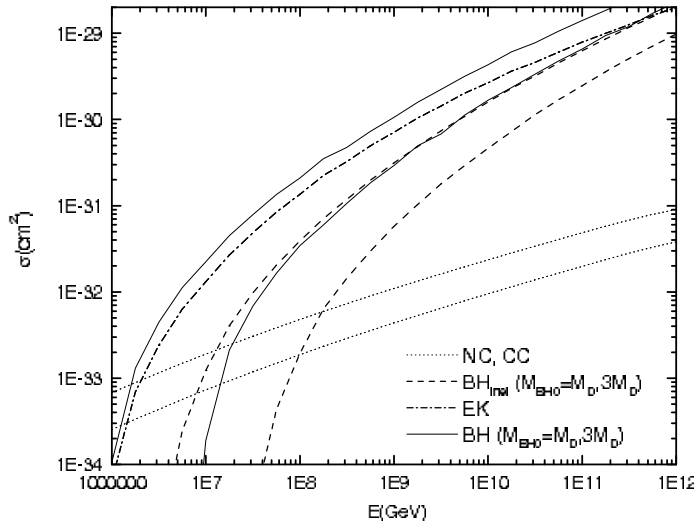


FIG. 1: Standard model and low scale gravity ( $M_D=1\text{TeV}$ ,  $d=6$ ) cross sections. Pair of dotted curves gives standard model NC (lower curve) and CC (upper curve) interactions. Pair of solid (dashed) curves gives black hole formation cross section, without (with) inelasticity, for  $M_{BH0}=M_D$  (upper solid (dashed) curve) and  $M_{BH0}=3M_D$  (lower solid (dashed) curve). The dash-dot curve is for graviton exchange case.

[24]. The cross section for this modeling of the impact-parameter effects reads

$$\sigma_{\nu N \rightarrow BH}(E_\nu) = \int_0^1 2z dz \int_{x_{min}}^1 dx \hat{\sigma}_{BH}(xs) \sum_i f_i(x, q). \quad (3)$$

Again,  $s = 2M_N E_\nu$  and  $E_\nu$  is the primary neutrino energy. All of the cross sections relevant in this paper are shown in Figure 1 for representative values of  $M_D$  and  $M_{BH0}$ , with  $d=6$ . The black hole production cross sections are sensitive to the values of  $M_D$  and  $M_{BH0}$  and to the inclusion of impact parameter effects. The bounds we obtain for  $d = 5$  or 7 differ by only five to ten percent from those obtained for  $d = 6$ , so we give details only for  $d = 6$  throughout. Laboratory and astrophysical data already place strong lower bounds on the cases  $d < 5$ .

We treat the graviton exchange in the higher dimension, low scale gravity picture in the eikonal approximation [25]. For more than 3 spatial dimensions, an impact parameter scale  $b_c$  enters the problem, and the dominant contribution to the eikonal amplitude when  $\sqrt{\hat{s}} \gg M_D$  comes from momentum transfer  $q = \sqrt{-(p - p')^2}$  in the range  $1/r_S > q > 1/b_c$ , where the stationary phase evaluation of the amplitude is a good approximation. The four momenta  $p$  and  $p'$  refer to the incident and scattered neutrinos respectively. The eikonal amplitude can be written in this approximation

$$|\mathcal{M}_d| = B_d (b_c M_D)^{d+2} [b_c q]^{-\frac{d+2}{d+1}}, \quad (4)$$

where  $B_d = 0.23, 0.039$  or  $0.0061$  when  $d = 5, 6$ , or  $7$ . The saddle point impact parameter reads  $b_c = \frac{1}{M_D} \left( \frac{s}{M_D^2} \right)^{\frac{1}{d}} \beta_d$ . The factor  $\beta_d = 1.97, 2.32$ , or  $2.66$  for  $d = 5, 6$ , or  $7$ . The elastic parton level cross section then reads,

$$\sigma_{EK}(x, q) = \frac{1}{16\pi xs} \sum_i f_i(x, q) |\mathcal{M}_d|^2,$$

which enters into the rate calculations below. The cross sections are displayed in Fig.1 for the case  $M_D = 1\text{TeV}$ .

At this point we can write the shower production rates for the eikonal and direct black hole production cases, specifying the restrictions on the range of integrations from impact parameter and threshold considerations. For the black hole production we have the folding of the neutrino flux energy distributions with the effective volume of the detector and the scattering cross sections on the nucleon target integrated over  $x$ . The eikonal set-up has an additional integration over the inelasticity parameter  $y$ . These expressions are presented below. These results have appeared in various forms elsewhere [26].

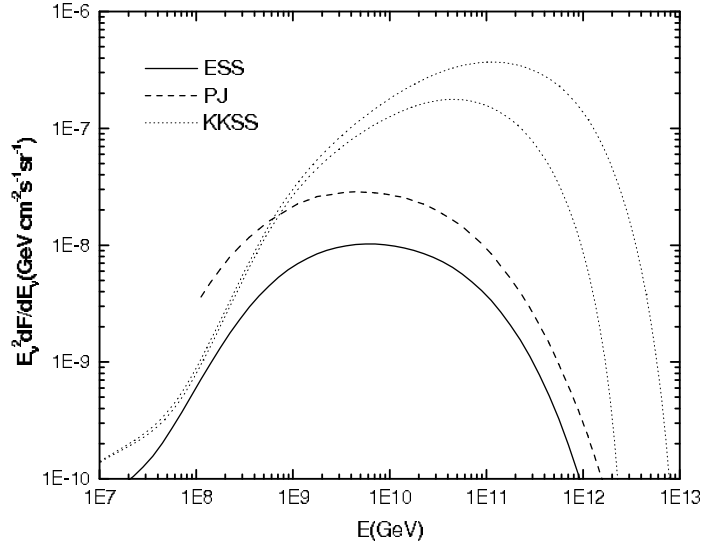


FIG. 2: Cosmogenic  $\nu_e$  fluxes by ESS [5], PJ [7], and KKSS [6]. We show the KKSS maximal and a relatively smaller flux for the KKSS case.

Shower rates from  $BH$  production and decay, with or without including the impact parameter effects (black hole inelasticity), are determined by folding the appropriate cross section with the effective volume and differential flux :

$$R_{shower}^{BH} = 2\pi\rho N_A \sum_i \int_{E_{th}}^{E_{\nu} \text{ max}} dE_{\nu_i} \frac{dF_i(E_{\nu})}{dE_{\nu}} V_{eff}(E_{\nu}) \sigma_{\nu N \rightarrow BH}(E_{\nu}), \quad (5)$$

where  $x_{\min} = M_{BH0}^2/s$  or  $1/r_s^2 s$ , whichever is larger, for the simple black disk case;  $x_{\min} = (M_{BH0})^2/M_{A.H.}^2(z)$  when the impact-parameter-dependent inelasticity estimate is included. The mass enclosed in the apparent horizon,  $M_{A.H.}$ , and the scaled impact parameter,  $z$ , are discussed above.  $E_{th}$  is the experimental threshold for detection of showers, taken to be  $100PeV$  for RICE. Above the cutoff  $E_{\nu}$  max, the integral gives negligible contribution to  $R$ . The rate shown is for down-going neutrinos, assuming an isotropic, diffuse flux of neutrinos, appropriate to those of cosmogenic origin. Fluxes are given per steradian, and the  $2\pi$  factor accounts for the integration of isotropic flux times angular average of the effective volume over the dome of the sky.

For the eikonal scattering case, the rate expression reads

$$R_{shower}^{EK} = 2\pi\rho N_A \sum_i \int_{E_{th}}^{E_{\nu} \text{ max}} dE_{\nu} \frac{dF_i(E_{\nu})}{dE_{\nu}} \int_{E_{th}/E_{\nu}}^1 dy V_{eff}(yE_{\nu}) \int_{M_D^2/ys}^{1/r_s^2 ys} dx \sigma_{EK}(x, q), \quad (6)$$

with  $q = \sqrt{ys}$ . The graviton exchange is affected only by the value of  $M_D$ , though there is an implicit dependence on the choice of minimum impact parameter where the eikonal, semiclassical approximation is expected to be valid. We have chosen this value as  $1/r_s$ . The fluxes we used to explore the range of event rates is shown in Fig. 2.

### III. NUMERICAL WORK AND RESULTS

To produce representative event rate predictions, we fix number of extra dimensions  $d$  at 6, consider both  $M_D = 1$  TeV and 2 TeV and the minimum BH mass values  $M_{BH0} = M_D$  and  $3M_D$ . As we noted in our outline of cross sections, changing  $d$  to 5 or 7 affects our bounds by only 5 - 10 percent. We use CTEQ6 [27] for the nucleon parton distributions. The cross sections for  $M_D = 1$  TeV are plotted from  $10^6 GeV$  to  $10^{12} GeV$  in Fig. 1.

When  $M_D = 2$  TeV, each cross section is reduced by roughly a factor 10. To assess flux model dependence on results, we chose large, medium, and small fluxes for comparison, as described in the caption of Fig. 2. We are primarily interested in cosmogenic flux models, generated by the GZK effect [5, 6, 7, 8]. These produce neutrinos at

TABLE I: 95% C.L. upper limit shower rates, for RICE 2000-2004 operation, in low scale gravity ( $M_D = 1$  TeV,  $d = 6$ ); rates are given for different cosmogenic neutrino flux models;  $BH$  and  $BH_{inel}$  give black hole formation rates (and hence shower rates) without and with inelasticity included, respectively; EK gives the shower rates due to graviton exchange. KKSS corresponds to the maximal flux case shown in figure 2.

Flux	SM	EK	BH1 ( $M_{BH_0} = M_D$ )		BH2 ( $M_{BH_0} = 3M_D$ )	
			$BH$	$BH_{inel}$	$BH$	$BH_{inel}$
ESS	0.1	0.66	38.4	4.0	15	1.4
KKSS	3.0	43	1509	238	697	98
PJ	0.27	1.7	106	11	41	3.7

the very highest energies, and are arguably less model-dependent than those generated from models of specific types of astrophysical sources. In Fig. 2 we show the comparison between the three flux models used, which show factors of three or more difference over most of the energy range of interest, and more than an order of magnitude in some regions [5, 6, 7, 8].

The qualitative features of our calculations in all channels can be anticipated from the power law growth of cross sections, times stronger power law fall of flux, times (slower) power law growth of effective volume to detect shower energy. The rapid decrease in flux with energy wins, but the growing cross sections and effective volume delay the loss of events as one scans higher and higher energies. In Table I we present the number of events expected in RICE over the 5 year period 2000-2004 using the three different cosmogenic flux models. We have integrated using an updated effective volume of the RICE detector [9] for our visible energy signal. In all cases  $E_{th}$  (our detector threshold) is  $10^7$  GeV. All rates are integrated over primary neutrino energy from threshold to the maximum energy where the flux cuts off. As shown in Table I, since at 95% C.L., with SM cross sections, the maximum number of events compatible with no background and zero observed events is 3.0, RICE nearly rules out the maximal KKSS cosmogenic flux model. The  $M_D = 1$  and  $d = 6$  choices made for Table I are irrelevant for the SM result, of course.

For the SM, EK and the direct BH production cases, the hadronic component of showers is assigned pulse strength equal to an electromagnetic shower of the same energy [28]. An important difference between electromagnetic and hadronic showers is that the hadronic showers do not suffer the loss of effective volume that is estimated to affect the electromagnetic showers due to the LPM [29] effect when computing event rates.

In the EK, BH1, and BH2 columns of Tables I and II, we show expected numbers of events in the RICE 2000-2004 data, with the acceptance (effective volume) and efficiencies in candidate event analysis included, coming individually from the eikonalized graviton exchange (EK), and black hole production processes. Representative scales  $M_D = 1, 2$  TeV are used, and for each the black hole formation thresholds  $M_{BH_0} = M_D, 3M_D$  are assumed and the black hole rate calculated. It is usually argued [13, 16] that in the range  $M_D < M_{BH_0} < 2M_D$ , the quantum gravity effects may dominate [30]; our point of view is that the new physics leading to shower formation will occur, and the EK and BH shower rates act as reasonable estimates of the enhancement in the transition region. Certainly one expects that the different energy regions tie together smoothly parametrically, and they do [30]. In addition we show two values of black hole events for each black hole  $M_D, M_{BH_0}$  parameter pair, corresponding to the simple “black disk” calculation and the calculation corrected for loss of efficiency for black hole formation when the impact parameter offset between neutrino and parton increases. The second number in the columns labeled “ $BH_{inel}$ ” is that obtained when the inelasticity effects are modeled as described above. The black hole ( $BH$ ) rates drop by an order of magnitude. The EK rate, unaffected by the  $BH$  inelasticity effects, is now about 20% of the  $BH_{inel}$  for  $M_{BH} = M_D$  case and 50% of  $BH_{inel}$  for the  $M_{BH}=3M_D$  case. Again this is true for all the flux models we apply, which cover a wide range of possibilities.

Pumping up the cross sections above SM extrapolations pushes harder on the flux bounds. Given that UHE neutrinos are not yet observed [9], choosing a flux model then allows one to limit cross sections, which predict at some point more events than current observational limits allow. For RICE, this number is 3.0 at 95% C.L., as noted earlier. Clearly most of the entries in Tables I and II are already disallowed at better than 95% C.L. To quantify this situation, we allow the mass scale of gravity to decrease (increase) and ask what value allows the event rate for a given flux to rise above (fall below) the 95% limit set by RICE. This value is what we quote in Table III and shown as a function of  $M_{BH_0}/M_{BH}$  in Fig. 3.

To assess the effect of BH inelasticity on  $M_D$  bounds, we also use the impact parameter dependent cross sections as modeled in [21, 24], to place bounds on  $M_D$  for each flux and  $M_{BH_0}$  choice. In Table III the  $BH$  and *ALL* columns again show two values each. The first refers to the case where all parton CM collision energy is available to the BH, while the second is the value after the modeling of inelasticity is included. The reduction in sensitivity to  $M_D$  is

TABLE II: Same as above with  $M_D = 2\text{TeV}$ .

Flux	EK	$BH1 (M_{BH_0}=M_D)$		$BH2(M_{BH_0}=3M_D)$	
		$BH$	$BH_{inel}$	$BH$	$BH_{inel}$
ESS	0.10	4.5	0.30	1.5	0.12
KKSS	7.2	195	29	78	10
PJ	0.26	12	1.2	4.0	0.32

TABLE III: Experimental lower bounds on LSG scale  $M_D$ , based on 2000-2004 RICE data (0 events, 0 background). Here ‘ALL’ is the combined bound due to  $EK$  and  $BH$ ; these bounds are due to all flavors. The pairs of numbers under columns  $BHD$  and ‘ALL’ are the bounds without and with black hole inelasticity, respectively. The bounds here include SM interactions. The numbers are in TeV. KKSS corresponds to the maximal flux case shown in figure 2. We fix number of extra dimensions  $d$  to 6. With  $d = 5$  or 7, we find values 2.0 TeV or 2.3 TeV instead of 2.15 TeV for the first entry in the ESS, BH slot in the table. These are typical fractional changes.

Flux	$M_{BH_0} = M_D$			$M_{BH_0} = 3M_D$	
	$EK$	$BH$	ALL	$BH$	ALL
ESS	0.55	2.15, 1.05	2.15, 1.1	1.55, 0.75	1.55, 0.85
KKSS	4.3	11, 6.0	11, 6.6	7.5, 4.0	7.9, 5.15
PJ	0.8	3.0, 1.45	3.0, 1.55	2.1, 1.05	2.15, 1.15

substantial, with reduction ranging from factors of 3/4 to 1/2.

Our results are summarized in Fig. 3, where we show the minimum value of the scale of gravity allowed by RICE data at 95% C.L. For a given case, the region *below* the curve is excluded. The points on the curves are obtained by setting the value of  $M_{BH_0}$ , and then varying  $M_D$  with  $d=6$  until the predicted number of events falls below 3, consistent with the RICE result of zero events on zero background at 95% C.L. The lower bound on  $M_D$  is plotted against  $M_{BH_0}/M_D$ , the ratio of a minimum invariant mass required for black hole formation to the scale of gravity. In setting the limit curves, the SM, LSG unitarized graviton exchange, EK, and the LSG black hole production cross sections, BH and  $BH_{inel}$ , are all included in determining event rates and, consequently, the bound. The top curve for each flux model represents the minimum  $M_D$  when the simple “black disk” model for the black hole formation cross section is used; the bottom curve indicates the lower limit when impact parameter dependence of the apparent horizon is included as estimated in [21] and implemented by [24]. The impact of the uncertainty in correct cosmogenic flux model and model of BH cross section on the bound of  $M_D$  is seen at a glance in Fig. 3. Fixing  $M_{BH_0}/M_D$ , the range of possible bounds on  $M_D$  follows by comparing the lowest curve to the highest.

#### IV. DISCUSSION OF RESULTS AND OUTLOOK

The essence of our results is shown in Fig. 3, where the region below a given curve shows the excluded region for which  $M_D$  is too small, and the LSG cross section too big, to be consistent with the RICE results [9]. As we comment further below, in connection with the information contained in the tables, the conclusions depend heavily on the flux model assumed and the treatment of the LSG interactions. It is clear that, should events be observed, there are likely to be a number of different parameter choices in the flux models and the cross section models that will reproduce the observed events.

Within the range of cosmogenic flux models we consider, Table III reveals that at 95 % C. L., RICE and the ESS flux model [5] rule out an LSG model where the naive  $\sigma_{BH} = \pi r_S^2$  cross section is assumed, where  $M_{BH} = 3M_D$ , and where  $M_D < 1.55$  TeV. This can be regarded as a least lower bound on models with the naive “black disk” cross section for the black hole formation within our analysis assumptions. The greatest lower bound corresponds to that obtained with the largest flux model, and the value is greater than 7.9 TeV (11 TeV) when  $M_{BH_0} = 3M_D$  ( $M_D$ ). The KKSS maximal flux model [6] is right at the borderline of our 95 % C.L. constraint using the SM cross section [9], so the corresponding LSG scale is imprecise. Basically there is no room for LSG if this flux model is assumed.

If the estimate of the effects of non-zero impact parameter are included in the manner proposed in [21], and some of the collision energy is lost to the BH formation process, then the BH formation cross sections decrease and the event

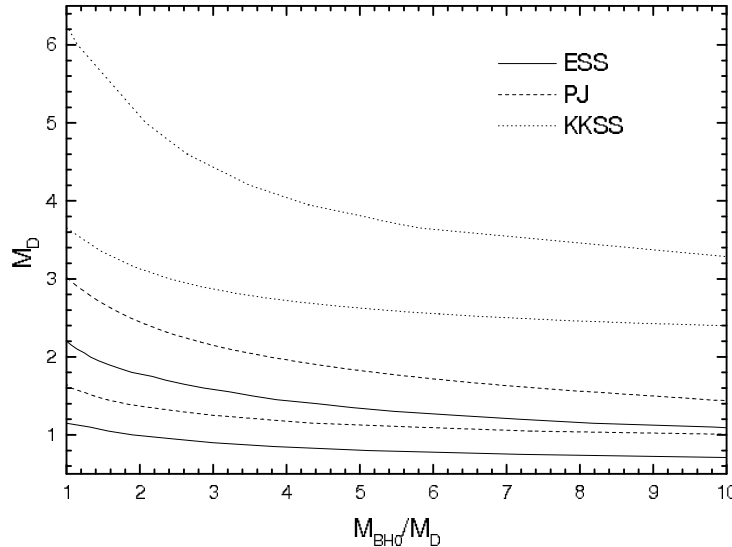


FIG. 3: Lower bounds on  $M_D$  as a function of the ratio of the minimum BH formation threshold,  $M_{BH0}$ , to  $M_D$ . The upper curve for each flux model is the lower bound when the naive, black disk model is used for the BH cross section. The lower curve is the lower bound when the estimate of impact parameter effects is included. ESS, KKSS (lower of the two KKSS curves in Fig.3) and PJ refer to Refs. [5], [6] and [7]

rates and corresponding bounds on the LSG scale weaken. The nominal effects on the least lower bound, tied to the flux model [5], and greatest lower bound, tied to KKSS [6] are the reductions to 0.85 TeV and 5.15, respectively. The greatest lower bound of all, 11TeV, occurs if the BH scale is equal to  $M_D$  and the simple black disk cross section is used with the maximum KKSS flux shown in Fig. 2. Given the lack of precision in these considerations, we summarize the most conservative bounds statement as an estimated range on the value of  $M_D$  as lying in the range between roughly 0.9 TeV and 10 TeV, as quoted in the Abstract.

Next, suppose for the sake of argument that a given number of events were actually observed in the RICE data. There are interesting degeneracies that occur. For example, there is an approximate degeneracy between the EK  $M_D = 1, 2$  TeV entries and  $BH$  ( $M_D = 1, 2$  TeV with  $M_{BH0} = 3$  TeV) entries for every flux model we used. The enhancements in event rates are more than an order of magnitude compared to SM in every case, but the interpretation, just within low scale gravity itself and with the flux known, will be a challenge. The *EK* calculation does not invoke black hole formation, but for one scale choice *EK* can yield the same signal enhancement as *BH* with a different scale choice.

When the extra uncertainties in flux are admitted, there is a sharp increase in the possible degeneracies in parameter choices, leading to similar event rates. For example, it is no surprise to find in Table III that the ESS flux with BH1 parameter choices give the same RICE event rate predictions as the PJ flux with the BH2 parameter set for the LSG model, with and without inelasticity included. Similarly, the PJ flux with EK interactions alone produce, as noted in Table III, the same bound on  $M_D$  as the ESS flux with ALL interactions included and inelasticity estimated for the BH production case.

A number of ideas have been proposed for distinguishing SM from new physics cross sections, and new physics cross sections from one another, independently of flux; see for example Ref. [26] and references cited there. Typically these ideas require angular information, at least number of up-going events vs. down-going events, to "divide out" the flux effects. To get discriminating power takes a sizable sample of events, which is a challenge for all UHE telescope projects.

These remarks remind us that the field of UHE neutrino telescope physics and astrophysics is still very young. All-in-all we are at a very complex, fluid and fascinating threshold of discovery. Much more experimental and theoretical work remains to be done.

**Acknowledgements** We thank Dave Besson and the RICE Collaboration for discussions and encouragement. Comments on early versions of the manuscript from Danny Marfatia are appreciated. John Ralston and Prasanta Das participated in the early stages of this work, and we thank them for their contributions. This work was supported in

part by the Department of Energy High Energy Physics Division and by the NSF Office of Polar Programs.

---

[1] T. Yamamoto, *Astropart. Phys.* **20**, 405 (2004); R.U. Abassi et al., *Astrophysical Journal* **610**, 173(2004). These are recent representative publications, where citations to details of the experiments can be found.

[2] K. Greisen, *Phys. Rev. Lett.* **16**, 748 (1966); G. Zatsepin and V. Kuzmin, *Pis'ma Zh. Eksp. Teor. Fiz.* **4**, 114 (1966) [JETP. Lett. **4**, 78 (1966)].

[3] V.S. Berezinsky and G.T. Zatsepin, *Phys. Lett.* **28B**, 423 (1969); F.W. Stecker, *Astrophys. J.* **228**, 919 (1979).

[4] N. Arkani-Hamed, S. Dimopoulos and G. Dvali, *Phys.Lett. B* **429** (1998) 263; I. Antoniadis, N. Arkani-Hamed, S. Dimopoulos and G. Dvali, *Phys.Lett. B* **463** (1998) 257.

[5] R. Engel, D. Seckel, and I. Stanev, *Phys. Rev. D* **64**, 093010 (2001).

[6] O. E. Kalashev, V. A. Kuzmin, D. V. Semikoz, and G. Sigl, *Phys. Rev. D* **66**, 063004 (2002).

[7] R. Protheroe and P. Johnson, *astro-ph/9506119*, *Astropart. Phys.* **4**, 253 (1996).

[8] Z. Fodor, S. D. Katz, A. Ringwald, and H. Tu, *hep-ph/0309171*, *JCAP* **0311**, 115 (2003).

[9] "Updated Limits on the Ultra-High Energy Neutrino Flux from the RICE Experiment", I Kravchenko et al., *Proceedings of the 29th International Cosmic Ray Conference* Pune (2005); "Using RICE Data and GZK Neutrino Flux Models to Bound Low Scale Gravity", I Kravchenko et al. *ibid.* "Updated Limits on the Ultra-High Energy Neutrino Flux from the RICE Experiment", in preparation.

[10] G. A. Askar'yan, *Zh. Eksp. Teor. Fiz.* **41**, 616 (1961) [Soviet Physics JETP **14**, 441 (1962)] and **48**, 988 (1965) [**21**, 658 (1965)]; M. Markov and I. Zheleznykh, *Nucl. Instrum. Methods Phys. Res. Sect. A* **248**, 242 (1986); J. P. Ralston and D. W. McKay, *Astrophysics in Antarctica*, AIP Conf. Proc. No. 198, edited by K.J. Mullan, M. A. Pomerantz, and T. Stanev (AIP, New York, 1989), p. 24; E. Zas, F. Halzen, and T. Stanev, *Phys. Rev. D* **45**, 362 (1992); A. L. Provorov and I. Zheleznykh, *Astropart. Phys.* **4**, 55 (1995); G.M. Frichter, John P. Ralston and D.W. McKay, *Phys. Rev. D* **53**, 1684 (1996).

[11] RICE Collaboration, I. Kravchenko et al., *Astroparticle Physics* **19**, 15 (2003); *Astroparticle Physics*, **20**, 195 (2003).

[12] The RICE collaboration, I. Kravchenko et. al. in proceedings of 28th ICRC, Tokyo, 2003 (Universal Academy Press, Tokyo, 2003).

[13] T. Banks and W. Fischler, *hep-th/9906038*; R. Emparan, G. Horowitz, and R. Meyers, *Phys. Rev. Lett.* **85**, 499 (2000).

[14] P. Argyres, S. Dimopoulos, and J. March Russel, *Phys. Lett. B* **441**, 96, (1998).

[15] S. Hawking, *Commun. Math. Phys.* **43**, 199 (1975).

[16] S. Dimopoulos and G. Landsberg, *Phys. Rev. Lett.* **87**, (2001) 161602; S. Giddings and S. Thomas, *Phys. Rev. D* **65**, 056010 (2002).

[17] K. Cheung, *Phys. Rev. Lett.* **88**, 221602 (2002); T. Rizzo, *hep-ph/0111230*; A. Ringwald and H. Tu, *Phys. Lett. B* **525**, 135 (2002).

[18] G. Domokos and S. Kovács-Domokos, *Phys. Rev. Lett.* **82**, 1366 (1999); S. Nussinov and R. Shrock, *Phys. Rev. D* **59**, 105002 (1999); P. Jain, D. McKay, S. Panda and J. Ralston, *Phys. Lett. B* **484** 267 (2000).

[19] J. Feng and A. Shapere, *Phys. Rev. Lett.* **88**, 021303 (2002); A. Anchordoqui and H. Goldberg, *Phys. Rev. D* **65**, 047502 (2002); A. Ringwald and H. Tu, *Phys. Lett. B* **525**, 135 (2002); M. Kowalski, A. Ringwald and H. Tu, *Phys. Lett. B* **529** 1 (2002); L. Anchordoqui, J. Feng, H. Goldberg and A. Shapere, *Phys. Rev. D* **66**, 103002 (2002).

[20] P. Kanti and J. March Russell, *Phys. Rev. D* **66**, 024023 (2002); *ibid* **67**, 104019 (2003).

[21] H. Yoshino and Y. Nambu, *Phys. Rev. D* **66**, 065004 (2002); *ibid* **67**, 024009 (2003).

[22] S. Giddings and S. Thomas, *Phys. Rev. D* **65**, 056010 (2002); H. Yoshino and Y. Nambu, *Phys. Rev. D* **66**, 065004 (2002); *ibid* **67**, 024009 (2003); E. J. Ahn, M. Ave, M. Cavaglia, and A. V. Olinto, *Astropart. Phys.* **22**, 377 (2005).

[23] R. Meyers and M. Perry, *Ann. Phys. (N.Y.)* **172**, 304 (1986).

[24] L. Anchordoqui, J. Feng, H. Goldberg and A. Shapere, *Phys. Rev. D* **68**, 104025 (2003); L. Anchordoqui, J. Feng, H. Goldberg and A. Shapere, *Phys. Lett. B* **594**, 363 (2004).

[25] R. Emparan, *Phys. Rev. D* **64**, 0204025 (2001); R. Emparan, M. Masip and R. Rattazzi, *Phys. Rev. D* **65**, 064023 (2002); G. Giudice, R. Rattazzi and J. Wells, *Nucl. Phys. B* **630**, 293 (2002); P. Jain, D. McKay, S. Panda and J. Ralston, *Phys. Rev. D* **66**, 065018 (2002); S. Hussain and D. McKay, *Phys. Rev. D* **69**, 085004 (2004).

[26] S. Hussain and D. McKay, *Phys. Rev. D* **69**, 085004 (2004); P. Jain, D. McKay, S. Panda and J. Ralston, *Phys Rev. D* **66**, 065018 (2002).

[27] H. L. Lai et. al. *Phys. Rev. D* **55**, 1280 (1997); J. Pumplin et al. *JHEP* 0207, 012 (2002); D. Stump et al. *JHEP* 0310, 046 (2003).

[28] S. Hussain and D. McKay, *Phys. Rev. D* **70**, 103003 (2004).

[29] Landau, Pomeranchuk and Migdal.

[30] R. Emparan and S. Dimopoulos, *Phys. Lett. B* **526**, 393 (2002). G. Guidice, R. Rattazzi, and J. Wells, *Nucl. Phys. B* **630**, 293 (2002).